SF2A 2013
L. Cambrésy, F. Martins, E. Nuss and A. Palacios (eds)

SIMULATIONS OF THE BARYONIC ACOUSTIC OSCILLATIONS 21 CM SIGNAL DURING THE REIONIZATION

Dominique Aubert [1]

Abstract. The imprint of baryonic acoustic oscillations in the structure of the intergalactic gas is in principle detectable during the epoch of reionization, at $z > 6$. Using large scale cosmological simulations post-processed to take in account the impact of radiative transfer, we assess the redshift evolution of the 21 cm signal at the BAO scale, evolution that is driven by the birth of the first UV sources that convert the neutral emitting hydrogen into an ionized and non radio-emitting gas. We find that the modelisation and the properties of the sources and their radiation is crucial to this evolution and show for instance that the inclusion of preheating due to X-Rays has a strong impact on the 3D power spectrum of the 21 cm brightness temperature. Conversely, the detection (or the lack of) of BAOs could therefore provide a constrain on the nature of the sources during the EoR in addition to providing a new range of redshifts to use the oscillations as cosmological standard rulers.

Keywords: Reionization, Numerical Simulation, Cosmology

1 Introduction

The epoch of reionization saw the hydrogen content of the Universe returning to an ionized state after a brief period when it was predominantly neutral after the Recombination. The process is thought to have ended at $z \sim 6$ as probed by quasar spectra, culminating with a quick transition where a network of HII regions overlapped rapidly, driven by a growing number of UV sources. This epoch can be probed via the redshifted 21 cm signal by the current and next generation of large radio observatories, where facilities such as SKA promise to be able to track the evolving topology of the neutral hydrogen as it disappears during the reionization.

As explained in the next section, the 21 cm signal is modulated by the neutral state of the hydrogen, its temperature and of course the underlying density distribution. On scales larger than, say, 100 comoving Mpc, and at this epoch ($z > 6$), this distribution still evolves linearly and therefore still contains the signature of the baryonic acoustic oscillations (BAOs hereafter) that were frozen in the cosmic gas distribution at the recombination. This signal is detected in the CMB ($z \sim 1100$, e.g. Planck Collaboration et al. (2013)), in the structure of the Lyman-alpha forest ($z \sim 2$, Busca et al. (2013)) and in the distribution of galaxies ($z \sim 0$, see e.g. Eisenstein et al. (2005)). Probing this signal during the reionization epoch ($20 < z < 6$) would therefore open a new window for the study of the BAOs, and strengthen their position as a multi-epoch cosmological probe.

However, the emissivity of the gas evolves as HII regions appear, grow and overlap. One can therefore ask, how effectively large is the redshift window of observation ? Previous studies on the subject are not fully conclusive (see e.g. Mao & Wu 2008; Rhook et al. 2009). It is found that BAOs can be detected until z=6-8 when ionized fraction can be as high as 10%. However, such studies often rely on simple analytic or semi-analytic reionization models and neglect for instance the fluctuations induced by the non-uniform X-ray background that could be important to forecast the 21 cm signal of neutral hydrogen (see e.g. Baek et al. (2010)).

In the current work, we aim at investigating this subject using numerical simulations of the reionization at high resolution. The gas and source evolution are provided by hydrodynamical simulations whereas the multi-frequency radiative transfer is performed as a post-processing step. Simulation outputs provide the ingredients for a simple modeling of the 21 cm signal that we analyze by estimating its power spectrum. Even though this work has been triggered with SKA in mind, we focused on the intrinsic detectability of the BAO features, without considering instrumental effects at the current stage even though they will *in fine* put additional limitations on their observation.

[1] Observatoire Astronomique de Strasbourg, UMR 7550, CNRS, Universite de Strasbourg

2 Methodology

The gas distribution is provided by a cosmological simulation performed by the adaptive mesh refinement (AMR) code RAMSES (Teyssier 2002). The box size is $1h^{-1}$ Gpc and sampled by 2048^3 coarse cells. Initial conditions were generated with Mpgrafic (Prunet et al. 2008), using WMAP-9 cosmological parameters (Hinshaw et al. 2013) and the transfer function of Eisenstein & Hu (1998). 3 additional levels were triggered by the AMR ensuring a 16384^3 formal resolution. Even though BAOs are large scale features, the high number of coarse resolution elements and the finer levels allow to reduce the impact of resolution on the simulated SFR. Star formation is performed on the fly using the implementation of Rasera & Teyssier (2006), with $\delta = 10$, an admittedly small value but necessary in such large scale simulated volume that is unable to capture small scale high density peaks. The simulation has been run down to $z = 5.3$ on 2048 cores of the Equipex Meso-center of the University of Strasbourg, providing 50 snapshots to cover the reionization epoch.

The hydrodynamical simulation being done, its outputs (star and density fields) were post-processed by the radiative transfer code ATON (Aubert & Teyssier 2008, 2010). This code uses a moment description of the radiative transfer equation, assuming an M1 closure relation between the radiative energy density and pressure. The transfer is performed for 3 groups of photons with typical energies equal to 18 eV, 200eV and 1 keV. The inclusion of large mean free path X-rays is important for the subsequent analysis: these high-energy photons are crucial to model the large scale reheating that occurs during the reionization and are therefore prone to affect the large scale 21cm signature of BAOs. The code also tracks the out-of-equilibrium ionization state and the cooling processes of hydrogen (only). ATON is fully ported on multi-GPU architecture, enabling x80 acceleration factors compared to CPUs : not only it allows us to use a simple (but conditionally stable) explicit scheme for the transport but also removes the necessity to use a reduced speed of light. In the current work, the 2048^3 density fields were averaged down to 512^3 cubes that were post-processed on 8 K20 Nvidia GPUs, also located at the Strasbourg University computing facility.

The source distribution is obtained from the distribution of stellar particles computed by the hydrodynamical simulation and their emissivity is set to achieve a reionization at $z \sim 6$: it should be noted that the star formation is far from being converged and the stellar particles therefore act merely as tracer of the geometrical distribution of stars. In the most simple fashion, each source is considered as an X-ray emitter, with 0%, 1% (being the most realistic see e.g. Glover & Brand (2003))or 10% of its luminosity emitted as X-rays and respectively labeled as UV, X and SX models. The stellar contribution to the source spectrum is assumed to be a 50000 K black body whereas the X-ray part is assumed ot be attached to a QSOs with a $\nu^{-1.6}$ spectral dependence. The resulting ionization histories for the 3 models are shown in Fig. 1 and can barely be distinguished. It illustrates the dominant role of UV photons over the X photons on the reionization process.

3 Results

The post-processing being completed, we have access to the evolution of ionization, temperature and density during the reionization. The 21 cm brightness temperature δT_b is provided by (Mellema et al. 2013) :

$$\delta T_b \sim 27 x_{\rm HI}(1+\delta)\sqrt{\frac{1+z}{10}\frac{\Omega_m}{0.27}}\left(1-\frac{T_{\rm CMB}(z)}{T_S}\right)\left(\frac{\Omega_b}{0.044}\frac{h}{0.7}\right)\left(\frac{1-Y_p}{1-0.248}\right)\left(1+\frac{1}{H(z)}\frac{dv}{dr}\right)^{-1} \text{mK} \qquad (3.1)$$

In the current work, we approximate the spin temperature T_S by the kinetic one. The 21 cm maps are analyzed in Fourier space using the 3D power spectrum $P_{\delta T \delta T}(k)$ defined as

$$\langle \delta T_b(\mathbf{k}, z)\delta T_b(\mathbf{k}', z)\rangle = (2\pi)^3 P_{\delta T \delta T}(k, z)\delta_D(\mathbf{k}-\mathbf{k}'). \qquad (3.2)$$

We show in Figure 1, the redshift evolution of $\Delta^2(k) = k^3 P_{\delta T \delta T}(k)/(2\pi)^3$ for the UV model, i.e. without any contribution from the X-rays. Clearly, BAOs can be detected until $z \sim 10$, corresponding to an ionized fraction of 1% in our simulations. The signal disappears as a high frequency feature kicks in at $k \sim 0.2$ Mpc^{-1}, driven by the rise of a network of small HII regions.

In Figure 2, we present $\Delta^2(k)$ for the 3 models at 4 different redshifts. At early times, all model present clear BAOs signatures. However, the approximation $T_S \sim T_K$ is likely to be crude at the initial stages of reionization when the Ly-α coupling is weak and so would our 21cm forecast. Later on, significant differences can be spotted between our different source models. Again, the UV model exhibit baryon wiggles at any time within this redshift range, whereas X-ray models present strong features at low spatial frequencies. They are induced by large scale temperature fluctuations, on larger distances than the ionization fronts. In the case of

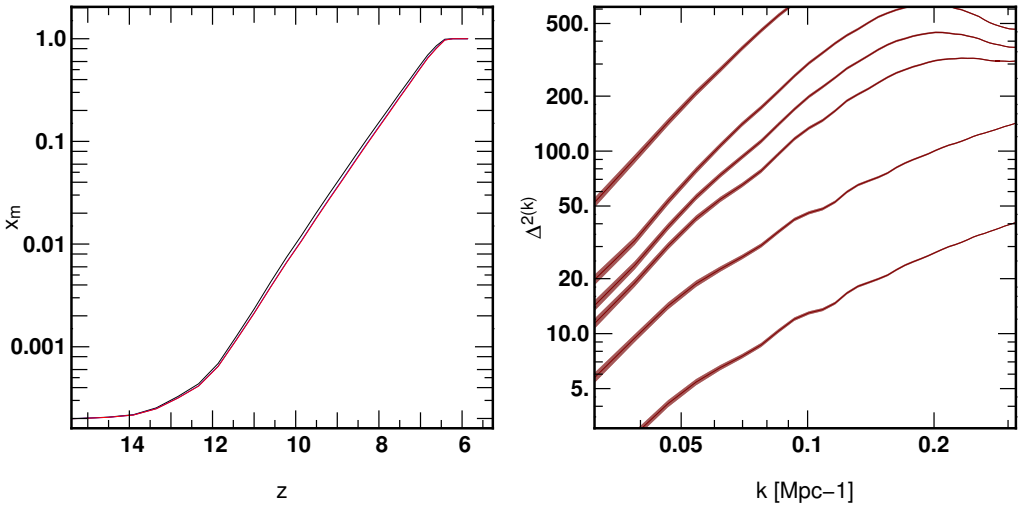

Fig. 1. Left: redshift evolution of the neutral fraction for the UV, X and SX models. Full reionization is achieved by $z \sim 6.5$ and the three models provide indistinguishable average reionization histories.**Right** measurement of the δT_b power spectrum $\Delta^2(k)$ in the UV model at z=15.8, 12.33, 10.6,10.2,9.85 and 9.18 (from bottom to top), corresponding to mass weighted neutral fractions of 0.0002, 0.0004, 0.0047, 0.006, 0.01 and 0.03. BAOs features can be distinguished on large scales until $x_m \sim 1\%$.

the SX model (corresponding to a 10 % luminosity in X-rays), the BAOs are drowned in this feature as soon as $z \sim 14$ ($x \sim 0.02\%$), while the X model is less dramatic even though the BAOs are washed out by $z \sim 12$ ($x \sim 0.06\%$). In general the X model present its large scale feature at higher frequency than for the SX model: soft-X rays seem to be the dominant source of large scale heating for the X model whereas harder photons contribute more efficiently in the SX one, with larger mean free path.

Qualitatively, these results are not surprising : X-rays have large mean free paths and their impact on large scale reheating can be important for the modeling of 21 cm signal. As a consequence, a large scale modification of the signal compared to a simulation devoid of X-rays is normal. Quantitatively, a mean free path of 300 h^-1 Mpc is expected for the hardest photons of our model, i.e. a length scale commensurable with the BAO scale. Still, one could have naively expected that a uniform temperature background would have been set rapidly thus reducing the impact of temperature fluctuations: this would have been an appropriate approximation for smaller scales, but generally not for the ones considered here. Still, one can note that a high frequency wiggle can still be distinguished in the SX model when z=11.5 : this scale would be small enough compared to the temperature fluctuation ones but its significance remain to be thoroughly investigated. Overall these simulations emphasize the relevance of a proper modeling of high-energy photons: a crude modeling (as the one described here) can erase this signature, hence the need for an accurate description of the amplitude of this contribution and the way it rises.

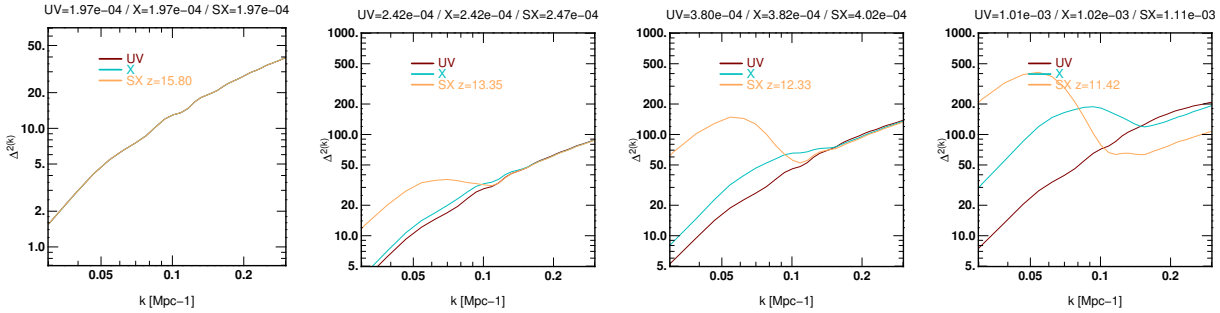

Fig. 2. Evolution of the temperature brightness power spectrum $\Delta^2(k)$ for the UV, X and SX models at 4 different redshifts. Neutral fractions are also provided for reference above the frames.

4 Discussion & Prospects

At this stage, our protocol must be considered as exploratory: X-ray source models, resolution issues, 21 cm modeling or the statistical treatment of the signal to name a few can all be debated. Rather than aiming at a definitive and quantitative answer, this work points toward issues that should be systematically treated in future, more complete investigations. Still, these preliminary investigations seem to imply that there is a possibility that BAOs should be detected behind a fluctuating 'foreground' generated by the heating sources of reionization. On the one hand, we have a weak signal, the BAOs, where their exact location in frequency space is known and on the other hand complex temperature fluctuations that are triggered by the source distribution and properties.

Let us finally note that spotting the oscillations could be an ideal application of the power spectrum decomposition suggested by e.g. Barkana & Loeb (2005):

$$P(k,\mu,z) = P_{\mu^0}(k,z) + \mu^2 P_{\mu^2}(k,z) + \mu^4 P_{\delta\delta}(k,z) \tag{4.1}$$

where μ is the cosine of the angle between the light of sight and $\mathbf{k}$ and appears because of the last velocity term in equation 1. It should be noted, that on scales considered here, the dynamics is close to linear and the velocity field can easily be computed from the density field, even though we have access to the self-consistent velocity provided by the simulations. By fitting $P(k,\mu,z)$ with a fourth order polynomial, the 'pure' density power spectrum $P_{\delta\delta}(k,z)$ that contains the BAOs can be recovered from the highest order term. Our preliminary investigations show that this decomposition can indeed provide the density structure below the features induced by the X-ray fluctuations but on scales, typically 50 Mpc, smaller than the one of interest. At the current stage we may be limited by the cosmic variance effect at the BAO scale, which is increased when one consider the line-of-sight dependence of the power spectrum instead as the usual averaged one. As a consequence, our simple polynomial fits on these scales are poorly constrained. Larger simulations are underway to see if this effect is dominant or if more subtle inversion procedure should be envisioned.

D.A. thanks B. Semelin for his insightful comments and direction. This work is supported by the ANR JCJC Grant EMMA. Simulations have been performed at the Mesocentre of the Universite de Strasbourg as part of the 2012 Meso Challenge.

References

Aubert, D. & Teyssier, R. 2008, MNRAS, 387, 295
Aubert, D. & Teyssier, R. 2010, ApJ, 724, 244
Baek, S., Semelin, B., Di Matteo, P., Revaz, Y., & Combes, F. 2010, A&A, 523, A4
Barkana, R. & Loeb, A. 2005, ApJ, 624, L65
Busca, N. G., Delubac, T., Rich, J., et al. 2013, A&A, 552, A96
Eisenstein, D. J. & Hu, W. 1998, ApJ, 496, 605
Eisenstein, D. J., Zehavi, I., Hogg, D. W., et al. 2005, ApJ, 633, 560
Glover, S. C. O. & Brand, P. W. J. L. 2003, MNRAS, 340, 210
Hinshaw, G., Larson, D., Komatsu, E., et al. 2013, ApJS, 208, 19
Mao, X.-C. & Wu, X.-P. 2008, ApJ, 673, L107
Mellema, G., Koopmans, L. V. E., Abdalla, F. A., et al. 2013, Experimental Astronomy, 36, 235
Planck Collaboration, Ade, P. A. R., Aghanim, N., et al. 2013, ArXiv e-prints
Prunet, S., Pichon, C., Aubert, D., et al. 2008, ApJS, 178, 179
Rasera, Y. & Teyssier, R. 2006, A&A, 445, 1
Rhook, K. J., Geil, P. M., & Wyithe, J. S. B. 2009, MNRAS, 392, 1388
Teyssier, R. 2002, A&A, 385, 337